

# Implementation of QR Decomposition for MIMO-OFDM Detection Systems

Kuang-Hao Lin, Robert C. Chang, *Member, IEEE*, Chien-Lin Huang, Feng-Chi Chen, and Shih-Chun Lin

Department of Electrical Engineering  
National Chung Hsing University  
Taichung, Taiwan  
89364306@ee.nchu.edu.tw

**Abstract**—An improved implementation of QR decomposition for MIMO-OFDM detection based on the Givens rotation method is presented in this paper. The hardware of QR decomposition is constructed by coordinate rotation digital computer (CORDIC) operating with fewer gate counts and lower power consumption than triangular systolic array structures. In wireless communication systems, the accuracy for transmitting signals is essential. Thus, a better data detection algorithm and precise channel estimation method plays an important role here. The channel estimation implemented with QR decomposition is to reduce hardware complexity of MIMO-OFDM detection. The results of implementation reveal that the proposed QR decomposition architecture has shorter clock latency than folding structure and smaller hardware area than Gram-Schmidt.

## I. INTRODUCTION

A recent surge of research on wireless local area networks (WLANs) has given us new challenges and opportunities. With the increasing usage of wireless communication systems, reliability requirements for high data rate have become more critical. In view of this, IEEE 802.11n system is based on the multiple input multiple output (MIMO)-orthogonal frequency division multiplexing (OFDM) technology [1], [2]. The advantages of MIMO-OFDM are as follows: more efficiently use of bandwidth, can combat the ISI effect and multi-path effect. Therefore, it is the current trend of WLANs by using MIMO-OFDM technology.

The detection algorithm technique for MIMO-OFDM wireless communication systems increases spectral efficiency. However, its complex receiver makes it unsuitable for low-complexity VLSI implementation. To reduce the complexity of the detection, several alternative algorithms and architectures are proposed [3], [4]. Noh *et al.* [3] proposed a low-complexity hardware architecture for MIMO-OFDM symbol detectors. The detectors support two MIMO-OFDM schemes of space-frequency block code OFDM and space-division multiplexing OFDM in order to achieve higher performance and throughput. Sobhanmanesh *et al.* [4] offered

a near optimal algorithm for V-BLAST detection in MIMO wireless communication systems based on QR factorization. However, an efficient implementation of the detection requires QR decomposition to reduce the hardware complexity of the MIMO-OFDM receiver.

The related works reported in the QR decomposition architecture can be classified into two major categories for hardware implementation. The first category is a parallel architecture based on modified Gram-Schmidt (MGS) algorithm [5], [6]. The other category is the triangular systolic array based on coordinate rotation digital computer (CORDIC) algorithm [7], [8]. However, within the extensive literature on QR decomposition, comparatively little research has focused on the relationship between clock latency and hardware area.

In this paper, we have proposed an improved QR decomposition hardware architecture based on Givens rotation method for MIMO-OFDM detection systems. In hardware point of view, the improved QR decomposition method is constructed using CORDIC algorithm with fewer gate count and lower power consumption than triangular systolic array structures. The QR decomposition architecture uses the iteration operation to reduce hardware complexity via vectoring mode and rotating mode circuits. Simulation results show the performances of QR decomposition with different iteration numbers.

This paper is organized as follows. Section II discusses the MIMO-OFDM detection systems. In section III, we present the efficient QR decomposition architecture. In Section IV, the simulation and implementation results are presented. Conclusions are drawn in Section V.

## II. MIMO-OFDM DETECTION SYSTEMS

To increase the data rate of the wireless communication, the spatial multiplex is used in the MIMO system with  $N_t$  transmitted antennas and  $N_r$  received antennas. Assuming that the signal  $x^i(t)$  represents the  $i$ -th of  $N_t$  transmitted vector pass through the channel response  $N_r \times N_t$  matrix  $\mathbf{H}$ , which is

---

This work was supported in part by the National Science Council (NSC), Taiwan, R.O.C. under Grant NSC 96-2220-E-005-004 and in part by the Ministry of Education, Taiwan, R.O.C. under the ATU plan. The authors would like to thank the National Chip Implementation Center (CIC) of Taiwan for technical support.

dependent on the transmitted angle, the incidences of received antennas, the number of multi-path in varied channel.

The main functionality of OFDM system is to ease the frequency selection effect. After FFT block as shown in Fig. 1, the received signals at the  $k$ -th subcarrier  $\mathbf{X}_k(n)$  can be obtained in frequency domain, as indicated in Eq. (1).

$$\mathbf{Y}_k = \mathbf{H}_k \mathbf{X}_k + \mathbf{n}_k, \quad \text{for } k=1, 2, \dots, N \quad (1)$$

The MIMO system is presented as Eq. (1) with  $N_t$  transmitted antennas and  $N_r$  received antennas, and the QR decomposition of  $\mathbf{H}_k$  is derived from computing the known preambles or known training sequences of wireless communication system by channel estimation in Fig. 1.

The received signal  $y$  in Eq. (1) can be modified by  $\mathbf{Q}^H$  to get

$$\begin{aligned} \hat{\mathbf{y}} &= [\hat{y}_1 \ \cdots \ \hat{y}_{N_r-1} \ \hat{y}_{N_r}]^T = \mathbf{Q}^H \mathbf{y} \\ &= \mathbf{Q}^H \mathbf{Q} \mathbf{R} \mathbf{s} + \mathbf{Q}^H \mathbf{n} = \mathbf{R} \mathbf{s} + \mathbf{Q}^H \mathbf{n} \\ &= \begin{bmatrix} r_{1,1} & \cdots & r_{1,N_r-1} & r_{1,N_r} \\ \mathbf{0} & \ddots & \vdots & \vdots \\ \vdots & & r_{N_r-1,N_r-1} & r_{N_r-1,N_r} \\ \mathbf{0} & \cdots & \mathbf{0} & r_{N_r,N_r} \end{bmatrix} \begin{bmatrix} s_1 \\ \vdots \\ s_{N_r-1} \\ s_{N_r} \end{bmatrix} + \begin{bmatrix} n_1 \\ \vdots \\ n_{N_r-1} \\ n_{N_r} \end{bmatrix} \quad (2) \end{aligned}$$

### III. QR DECOMPOSITION DESIGN

Nowadays, most of the modern MIMO-OFDM data-detecting methods are combined with QR decomposition algorithm [1]–[4]. The main reason is that, after QR decomposing the channel response, we not only can keep the data orthogonal, but also can simplify the procedure of signal processing. When the channel response  $\mathbf{H}$ , is QR decomposed, it will be transformed into an up-triangular matrix  $\mathbf{R}$ . Therefore, the interference of every received signal is reduced. Since using QR decomposition algorithm can decrease the complexity of equalizer, the total size will not be increased due to the additional QR decomposition.

The common QR decomposition algorithms are Gram-

Schmidt orthogonalization [5], Givens rotation [7], Householder transformation, etc. Since Householder transformation is much more complex in hardware implementation than the other two algorithms, we will only discuss the Givens rotation with CORDIC method in this paper.

#### A. CORDIC Method

##### 1) Vectoring Mode

In QR decomposition, by using vectoring mode of CORDIC, we can convert the complex numbers of input matrix into real numbers and do row cancellation, so as to produce the R matrix of QR (an up-triangular matrix, all of whose diagonal elements are real numbers). Mathematically, assume that input is equal to  $x+iy$ , using vectoring mode of CORDIC is to eliminate  $y$ . In other words, we can use each calculated value  $y$  to control the direction of rotation. The vectoring equation is given by

$$\begin{cases} x_{i+1} = x_i - y_i \cdot d_i \cdot 2^{-i} \\ y_{i+1} = y_i + x_i \cdot d_i \cdot 2^{-i} \\ z_{i+1} = z_i + d_i \cdot \tan^{-1}(2^{-i}) \end{cases} \quad \text{where } \begin{cases} d_i = 1, & y_i < 0 \\ d_i = -1, & \text{otherwise} \end{cases} \quad (3)$$

After several iterations, we can get  $y=0$ , and new coordinates  $(x', 0)$  with a rotational angle  $z$ .

##### 2) Rotating Mode

Rotating mode is to make a coordinate rotate a given angle or to make two coordinates rotate the same angle. For QR decomposition, the rotating angle  $z$  produced by vectoring mode is transmitted other elements of the same row for coordinate rotation. We can control the direction of rotation with every calculated value of  $z$ . The rotating equation is given by

$$\begin{cases} x_{i+1} = x_i - y_i \cdot d_i \cdot 2^{-i} \\ y_{i+1} = y_i + x_i \cdot d_i \cdot 2^{-i} \\ z_{i+1} = z_i - d_i \cdot 2^{-i} \end{cases} \quad \text{where } \begin{cases} d_i = -1, & z_i < 0 \\ d_i = 1, & \text{otherwise} \end{cases} \quad (4)$$

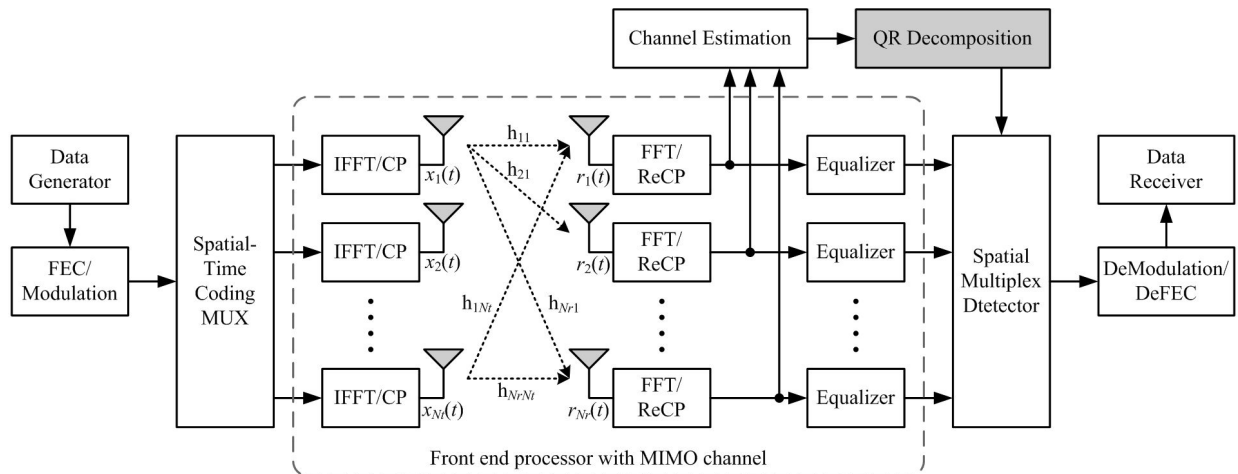


Figure 1. The block diagram of a spatial multiplex MIMO-OFDM wireless communication system.

After several iterations, we can get  $z=0$  and new coordinates  $(x', y')$ , which is the result of rotating the angle  $z$ . No matter in the vectoring mode or the rotating mode, there will always be the maximum angle restriction, and the range is  $-\pi/2 \sim \pi/2$ . If the angle exceeds the maximum value that  $\tan\theta$  can represent, it may result a wrong calculation. Therefore, we have to rotate the coordinates on the second and the third quadrants to the first and the forth quadrants by Eq. (5).

$$\begin{aligned}
 d &= -\text{sign}(y_i) & d &= \text{sign}(z_i) \\
 x_{\text{initial}} &= -d \cdot y_i & x_{\text{initial}} &= -d \cdot y_i \\
 y_{\text{initial}} &= d \cdot x_i & y_{\text{initial}} &= d \cdot x_i \\
 \underbrace{z_{\text{initial}} = d \cdot \frac{\pi}{2}}_{\text{Vectoring Mode}} & & \underbrace{z_{\text{initial}} = z_i - d \cdot \frac{\pi}{2}}_{\text{Rotating Mode}} & 
 \end{aligned} \quad (5)$$

### 3) Architecture Design

Since the desired input rotational angle of rotating mode is obtained from the calculation result of vectoring mode. When the result comes out from vectoring mode operation, the system must generate an enable signal, and together with the calculated angle, send to rotating mode operation. When rotating mode receives the enable signal, it starts to operate. Besides, after rotation mode operation, an enable signal will be generated, which is used to start register file operation. Then, write the calculated result of rotating mode into the register file. The architecture of vectoring mode and rotating mode is shown in Fig. 2.

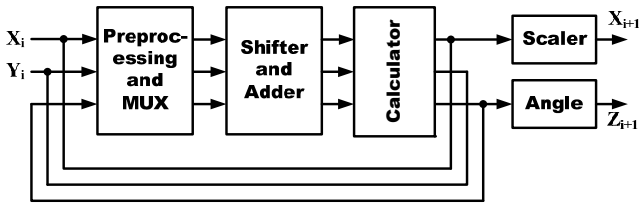


Figure 2. Vectoring Mode and Rotating Mode Architecture.

### B. Improved QR Decomposition Architecture

In this paper, we have proposed a modified QR architecture, as shown in Fig. 3. This architecture will increase CORDIC processing units, according to matrix expansion, but we don't need complex control circuit and rotating mode circuit. Thus, the area of a single CORDIC processing unit is smaller than that of the architecture introduced above. The single-port or dual-port register files generated by the Artisan Memory Generator are used as the storage unit. A register circuit is needed on every processing unit, but by the way, these can be shared with the previous stage (the channel response  $H$  estimated with storage channel). Therefore, we can save the hardware size of the receiver.

Since each CORDIC processing unit works independently, the register file of vectoring mode must be dual-port, so as to

avoid the two processing units, the vectoring mode and the rotating mode, from reading or writing the first register file at the same time, which may lead to wrong judgment. The vectoring mode and rotating mode are dual-input processing units originally. Here, we modify it to a single-input with the output feedback as the next input. After the first operation, an enable signal and a rotational angle will be sent to the rotating mode to start the operation. At this moment, the enable signal stimulates vector mode to read the next address data of register file, and then continue to do the following operations until it receives the disable signal given by the control circuit.

Because it is not necessary to determine whether to convert the real part or the imaginary part, the architecture of the control circuit is simpler. A vectoring mode control circuit uses two counters, i.e., one upper counter and one lower counter. The upper counter is controlled by processing units. When vectoring mode gets the result, it will send an enable signal to the next stage, and at this very moment, register file will be stimulated to do the reading and process the next row elements of matrix. The lower counter is an index counter. Its value is counted down from  $N$ , where  $N$  is the matrix dimension. When the values of the upper counter and the lower counter become the same, the lower counter will subtract 1, and the first row operation result will be sent out. The second row vector cancellation will proceed and so forth. When the values of the upper counter and the lower counter are both 2 at the same time, it will end the whole QR decomposition operation.

The design concept of the rotating mode control circuit is similar to that of the vectoring mode control circuit. The only difference is that the stimulating signal is sent after the operation of the rotating mode circuit. At the same time, the enable signal stimulates the last stage of register file and writes into the register. Each rotating mode processing unit works independently, but is synchronized. Therefore, all the rotating mode processing units can share the same control circuit.

Another advantage of using this improved architecture is low power consumption. Since each processing unit works independently and the necessary processing unit will become one less after each one-column vector processing, we can disable unused processing units and register files with gated clock, and the power consumption will be reduced.

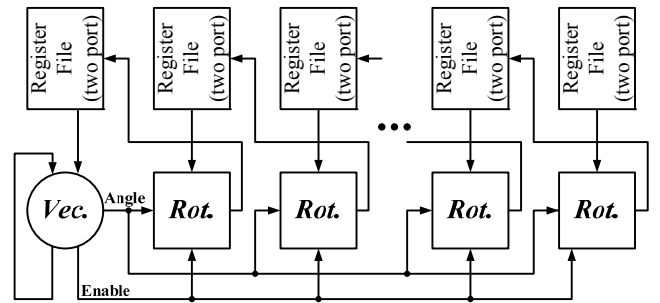


Figure 3. Improved QR decomposition architecture.

#### IV. SIMULATION AND IMPLEMENTATION RESULTS

The performance of MIMO-OFDM detection with the sphere decoding is shown in Fig. 4. The uncoded BER simulation result is appeared by the QR decomposition based on CORDIC with different iterations in 64-QAM and 4×4 MIMO system. The Rayleigh fading and the AWGN channel are employed for simulation. From Fig. 4, we can see that the curves of different iterations from 8 to 16 times are very close. For system application, making source accuracy in MIMO-OFDM detection, eight iterations of CORDIC computing is enough to execute the QR decomposition.

Fixed point simulation is performed to find the suitable number of bits for hardware implementation. Figure 5 shows that MSE is converged to  $10^{-3}$  when the number of bits is 8. While increasing the number of bits, the system performance will not be affected. Therefore, 8-bit fixed point is sufficient in this system. It is interesting to see from Fig. 5, when the wordlength of the system is  $N$ -bit,  $N$  iterations should be done for better performances.

Table 1 illustrates the comparison results of this work with the folding structure [4] and the Gram-Schmidt algorithm [5]. The processing matrix is increasing in the improved Architecture we proposed, but the characteristics of CORDIC recover the disadvantage of matrix expansion. Although the folding structure has fewer logic gates, the memory required is 4 times greater and clock latency is higher than the proposed structure. As given in Table 1, the proposed architecture has shorter clock latency than folding structure and smaller hardware area than Gram-Schmidt.

#### V. CONCLUSION

This paper has presented an improved implementation of the QR decomposition based on Givens rotation method for MIMO-OFDM detection systems in a wireless baseband receiver. The CORDIC architecture for the improved QR decomposition can efficiently reduce the hardware cost for wireless MIMO-OFDM detection systems, because the CORDIC architecture with vectoring and rotating modes doesn't require multiplications. The schedule of QR decomposition operation reduces clock latency and preserves precision for the performance of detection. The proposed architecture is implemented and verified by TSMC 0.13  $\mu\text{m}$  1P6M CMOS technology in the Rayleigh fading and AWGN, where the CORDIC is constructed by the 8-bit wordlength and the 8-time iteration.

#### REFERENCES

- [1] Jee-Hye Lee, Myung-Sun Baek, and Hyoung-Kyu Song, "Efficient MIMO Receiving Technique in IEEE 802.11n System for Enhanced Services," *IEEE Trans. Consum. Electron.*, vol. 53, pp. 344–349, May 2007.
- [2] Jaekyun Moon, Hui Jin, Taehyun Jeon, and Sok-Kyu Lee, "Channel estimation for MIMO-OFDM systems employing spatial multiplexing," in *Proc. IEEE Veh. Technol. Conf.*, pp. 3649–3654, Sept. 2004.
- [3] S. Noh, Y. Jung, S. Lee, and J. Kim, "Low-Complexity Symbol Detector for MIMO-OFDM-Based Wireless LANs," *IEEE Trans. Circuits Syst. II: Exp. Briefs*, vol. 53, pp. 1403–1407, Dec. 2006.
- [4] F. Sobhanmanesh, and S. Nooshabadi, "Parametric minimum hardware QR-factoriser architecture for V-BLAST detection," *IEE Proc. Circuits Devices Syst.*, vol. 153, pp. 433–441, Oct. 2006.

- [5] C.K. Singh, S.H. Prasad, and P.T. Balsara, "VLSI Architecture for Matrix Inversion using Modified Gram-Schmidt based QR Decomposition," in *Proc. Int. Conf. VLSI Design*, pp. 836–841, Jan. 2007.
- [6] C.K. Singh, S.H. Prasad, and P.T. Balsara, "A Fixed-Point Implementation for QR Decomposition," in *Proc. IEEE Dallas Workshop Design Applcat. Integration Software*, pp. 75–78, Oct. 2006.
- [7] A. Maltsev, V. Pestretsov, R. Maslennikov, and A. Khoryaev, "Triangular systolic array with reduced latency for QR-decomposition of complex matrices," in *Proc. IEEE Int. Symp. Circuits Syst.*, pp. 385–388, May 2006.
- [8] Zhaohui Liu, K. Dickson, and J.V. McCanny, "Application-specific instruction set processor for SoC implementation of modern signal processing algorithms," *IEEE Trans. Circuits Syst. I: Reg.Papers*, vol. 52, pp. 755–765, April 2005.

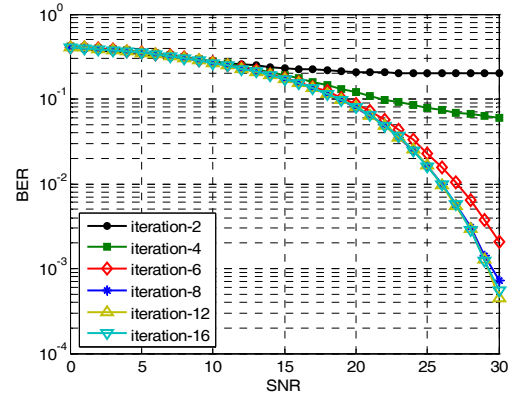


Figure 4. The performance of MIMO detection with different iterations.

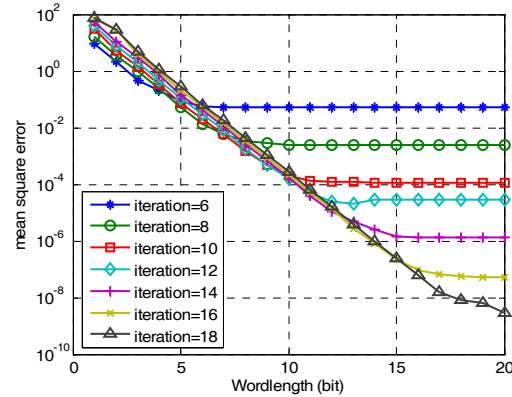


Figure 5. Fix Point Simulation.

TABLE I. COMPARISONS OF THE IMPLEMENTATION RESULTS

	This work	Ref.[4]	Ref.[5]
Algorithm	Given Rotation	Given Rotation	Gram-Schmidt
Order	8x8 (real)	4x4 (complex)	4x4 (real)
Clock Latency	88 clocks	252 clocks	67 clocks
Technology	0.13- $\mu\text{m}$ CMOS	FPGA	0.18- $\mu\text{m}$ CMOS
Gate Count	27k	about 6k	72k
Memory Require	1280bits	2416bits	None
Power	2.21mW	None	None